SSRG International Journal of Applied Physics
ISSN: 2350-0301/ https://doi.org/10.14445/23500301/IJAP-V9I3P105

Volume 9 Issue 3, 44-54, Sep-Dec 2022

Original Article

Effect of Doping and Co-sensitization on the Photovoltaic Properties of Natural Dye-sensitized Solar Cells

Okafor C. Emmanuel[1], Okoli N. Donald[2], Imosobomeh L. Ikhioya[3]

[1,2]*Department of Physics and Industrial Physics, Nnamdi Azikiwe University, Awka, Nigeria*
[3]*Department of Physics and Astronomy, University of Nigeria, Nsukka, Enugu State, Nigeria*

Received: 29 October 2022 Revised: 03 December 2022 Accepted: 16 December 2022 Published: 30 December 2022

Abstract *- The fabrication of dye-sensitized solar cells was successfully carried out using the Dr. Blade deposition method on transparent Fluorine-doped Tin Oxide (FTO) coated glass substrates with a sheet resistance of 16.6Ω/sq. The natural dyes used in this research were extracted from bitter leaf (chlorophyll pigment) (vernonia amygdalina), Zobo (anthocyanin pigment) (roselle) plant and a mixture of both dyes using ethanol as the extraction solvent. 50 g of each blended bitter leaf and zobo leaf were separately extracted in 250 ml of ethanol using a beaker. 25 g each of both dyes was adequately mixed and extracted in another 250 ml of ethanol inside a beaker. The cell was fabricated using lead as the counter electrode, nanocrystalline Titanium (IV) Oxide as the photoelectrode and potassium iodide as the electrolyte. 0.01 mol of hydrated nickel dichloride was used in doping the TiO_2 nanoparticles. The XRD pattern showed irregular polycrystalline thin films with fairly randomly oriented peaks. Intense and narrow peaks were seen at (110) and (311) orientation for the film corresponding to 2θ values of 25.34° and 68.77°, respectively. Optical characterizations of the fabricated cells were carried out using UV-Vis (UV-1800) spectrophotometer. It was seen that all the nickel-doped dyes showed a moderate absorption peak of 40% in the UV region of the electromagnetic spectrum. A solar simulator was used for the I-V characterizations of the fabricated cells at an illumination intensity of 881mW/cm^2. The combined chlorophyll and anthocyanin-based dyes, which gave the highest conversion efficiency of 1.63% and the least energy band gap of 1.92 eV, were seen to be more efficient than the two lone dyes with efficiencies of 0.31% and 0.40% for the anthocyanin and chlorophyll-based dyes respectively. The observed high efficiency of the co-sensitized dyes implies the dye synergic absorption effect due to co-sensitization. It also suggests that 0.01 mol of the nickel dopant increases the electrical characteristics of the combined dyes.*

Keywords *- Chlorophyll-based dyes, Bandgap, XRD, Doping, Efficiency.*

1. Introduction

The PV markets are dominated by photovoltaic (PV) modules based on silicon solar cells. This is due to its high efficiency and crystallinity (26.7 percent). However, to reach the high efficiency required by high pure silicon, a high vacuum and high-temperature system must be used, both of which are quite expensive [1]. In contrast to expensive conventional silicon solar cells, dye-sensitized solar cells (DSSCs) are quickly considered a source of future energy supply [2-4]. DSSCs are made of readily available, inexpensive, and ecologically benign materials. In recent years, numerous studies have been conducted on the fabrication of DSSCs with high performance, high reliability, higher efficiency, and low fabrication cost [5-7]. The DSSC investigation was influenced by photosynthesis, in which chlorophyll plays a significant role, in much the same manner that the dye harvests solar energy to facilitate charge transfer in DSSC [8]. Screen printing or inkjet, Doctor blade procedures, spray pyrolysis, sputtering, thermal oxidation, spin coating, hydrothermal method, electrochemical method, and SILAR techniques can all be used to create the promising DSSC [9–14]. How effective a DSSC is may depend on various material qualities, including the type of dye used, the photoelectrode material, the electrolyte type, and the counter electrode material. As an electrode material for DSSC, zinc oxide (ZnO) [15], tin oxide (SnO_2), niobium pentoxide (Nb_2O_5), etc., have all been used [16–20]. Compared to other photoelectrode materials, TiO_2 has achieved a maximum efficiency of roughly 14 percent and is widely employed by scientists [21]. TiO_2, in addition to having amazing qualities like environmental friendliness and affordability, is also chemically stable in solution when exposed to solar radiation, in contrast to CdS, InP, and GaAs materials, which putrefy in solution when light is shone on them.

Dye-sensitized solar cells (DSSCs) are gadgets that use inexpensive, non-toxic materials to convert solar radiation into electricity [22]. Environmental issues, including global

warming and the scarcity of fossil fuels, have made renewable energy more popular. Different kinds of solar cells have been created over time to convert sunlight into electricity. Solar cells made of crystalline, polycrystalline, and amorphous silicon, among others, have all been widely used in various commercial and home applications [23]. The difficulty in supplying energy is one of the biggest issues in the majority of developing nations. These issues resulted from the rapidly rising human population, the destruction of high-voltage power lines, the use of subpar equipment, and the neglectful maintenance of facilities. However, a consistent source of energy supply needs to be created to eliminate the problems that have been noticed. Both renewable and non-renewable energy sources exist. The energy obtained from renewable resources and used again is known as renewable energy [41]. These energies can be obtained from sun, wind, hydropower, biomass, and geothermal sources. They all create clean, economic, quiet, and simple energy to manufacture. Both renewable and non-renewable energy sources exist. The energy obtained from renewable resources and used again is known as renewable energy [25]. These energies can be obtained from sun, wind, hydropower, biomass, and geothermal sources. They all create clean, economic, quiet, and simple energy to manufacture [33-38].

Photovoltaics is the method of producing direct current electricity by converting solar energy into it using semiconductors (PV). Polycrystalline silicon, monocrystalline silicon, amorphous silicon, cadmium telluride, cadmium sulfide, copper-indium-gallium selenide, and copper-indium sulfide are the materials most commonly used nowadays in photovoltaics [26]. The most popular photosensitizers are synthetic dyes, which are very effective and have a magnificent capacity for light harvesting. However, due to their high cost, toxicity, and lack of availability, natural dyes have come to be seen as an alternative.

Due to their low cost, lack of noise, versatility, ease of extraction, abundance in nature, and environmental friendliness, dye-sensitized solar cells (DSSCs) are one of the most promising energy conversion technologies. This system, which uses a method akin to photosynthesis to generate electrical energy, was first described by [22]. Initially, dye sensitized solar cells (DSSCs) still used ruthenium-based dyes. But because ruthenium is rare and difficult to manufacture, scientists are starting to focus more on natural colours. Plants' leaves, flowers, and fruit can be utilized to color DSSCs.

The influence of doping and co-sensitization on the photovoltaic characteristics of dye-sensitized solar cells is presented in this study. As the extraction solvent, ethanol was used to extract the chlorophyll pigment from the bitter leaf (Vernonia amygdalina), the anthocyanin pigment from Zobo (Roselle), and a combination of both dyes. Using a beaker and 250 ml of ethanol, 50 g of mixed bitter and zobo leaf were extracted separately. Both dyes, 25 g each, were well combined before being extracted in a beaker with an additional 250 ml of ethanol. Cabon served as the counter electrode, nanocrystalline Titanium (IV) Oxide served as the photoelectrode, and potassium iodide served as the electrolyte in the construction of the cell. The doping was done using 0.01 mol of hydrated nickel dichloride.

2. Materials and Methods

For the creation of the naturally dye-sensitized solar cells, the following materials were used in this study: Vernonia amygdalina (bitter leaf), Zobo (roselle) plant, distilled water, and a substrate made of fluorinated tin oxide (FTO) with a sheet resistance of 16.6 ohms per square inch and a thickness of 3 mm. Titanium dioxide (Degussa P25), hydrated nickel dichloride, lead, ethanol, methanol, iodide electrolyte, filter paper, petridish, lab coat, masking tape, latex hand gloves, beaker, ceramic mortar and pestle, stirring glass rod, ultrasonicator (JL-60DTH), weighing scale, aluminum foil, sieve, temperature control furnace, detergent, and blender.

2.1. Dye Extraction from the Selected Samples

Samples of bitter leaf (chlorophyll pigment) and zobo (anthocyanin pigment) plants were harvested from the farm. The selected plants were first washed with ordinary water and then rinsed with distilled water. The samples were allowed to dry at room temperature for four days. The dried samples were then blended separately using a blender. The total mass of the grinded bitter leaf dye was measured to be 110.6 g using a chemical balance, while the total mass of the grinded roselle plant was 168.22g, and 50 g of the grinded bitter leaf was mixed with 250 ml of ethanol inside a beaker. The mixture inside the beaker was covered with aluminum foil, allowing one hour to extract the bitter leaf dye adequately.

Similarly, for the roselle plant, 50 g of the grinded roselle plant was mixed with 250 ml of ethanol inside another separate beaker. The beaker was also covered with a foil and allowed for one hour for proper extraction. The preparation of co-sensitizer involved the combination of bitter leaf and roselle plant. 25 g of grinded bitter leaf was mixed with another 25 g of grinded zobo plant, giving a total of 50 g. The combined dyes were mixed with 250 ml of ethanol and were allowed to extract for one hour. After one hour, the lone dye solution and the co-sensitized dye solution were filtered first with a sieve and then with filter paper. The filtrates were used as the photosensitizer.

2.2. Cleaning of FTO Glass Substrate

Fluorine-doped tin oxide (FTO: 16.6**Ω**/sq, 3mm thick, solaronix) glass was ultrasonicated for 30 minutes using ethanol and for another 30 minutes using distilled water to remove contaminants. The ultrasonicated substrates were dried under compressed hot air for 30 minutes at 60^{o}C using a furnace. The conductive side of the FTO substrate was determined using a digital multimeter (DT-830D).

2.3. Preparation of TiO_2 Colloidal Solution

The TiO_2 paste was prepared by gradually adding 15ml of methanol to 1gram of TiO_2 powder (Degussa P25) in a ceramic mortar and stirred thoroughly for about 45 minutes with a pestle to separate aggregate particles and achieve homogeneity. To produce a uniform and homogenous suspension, 1 ml of methanol was added, and the mixture was grinded before adding another 1ml of the solution. The process continued until the 15 ml of methanol solution was used up. The grinding and stirring process lasted for about 45 minutes. Dried particles of TiO_2 collected at the sides of the mortar and on the pestle were removed and returned to the center of the mortar using a flexible spatula. The processes continued until the deposition of the TiO_2 on the FTO substrate.

2.4. Doping of the TiO_2 Paste

0.01mol concentration of hydrated nickel dichloride ($NiCl_2 \cdot 6H_2O$) was prepared and used as the dopant. Nickel is a period 4 transition metal and is expected to improve the electrical conductivity of the solar cell. The 0.01mol concentration of the nickel dopant was completely dissolved in 2 ml of methanol inside a beaker

2.5. Deposition of the TiO_2 film on the FTO Substrate using the Dr. Blade method

The Doctor Blade method of deposition is employed here. Before the TiO_2 layer was deposited on the FTO substrate, a masking tape covering 0.15 to 0.2 cm of the FTO substrate was applied to the two parallel sides of the conducting face of all the FTO. The substrate for the deposition of TiO_2 paste was a transparent fluorine-doped tin oxide conducting glass with an average diameter of 2.35 cm by 2.50 cm. The masked edges were checked for gaps and openings using a glass rod. A glass stirring rod was used to disperse the material evenly on the FTO glass, gliding across the exposed area of the glass as the conducting face was facing upwards. A few drops of the TiO_2 solution were uniformly deposited on the substrate [26]. All deposited samples were given 45 minutes to dry at room temperature after being deposited. After carefully removing the Scotch tape, the electrode was sintered in a temperature-controlled furnace for 30 minutes at 450°C. To prevent cracking, the sintered TiO_2-covered conductive glass substrate was removed after a slow cooling process within the furnace. All of these actions were taken to improve mechanical and electrical adherence to the glass.

2.6. Dye Sensitization of the TiO_2 Deposited Substrates

Three sensitizers used are natural dyes extracted from bitter leaf (vernonia amygdalina), Zobo (roselle) plant, and the mixture of the two dyes in equal proportion. The dyes were poured into different beakers, and each working electrode was immersed inside the beakers containing the dyes. Before the immersion, the two parallel edges of the conducting face of all the working electrodes were again covered with scotch tapes to avoid dye impregnation around those areas. All the immersed working electrodes were faced inside the beaker to avoid scratching the TiO_2-deposited surface [27]. The impregnation process lasted for 24 hours for the dye molecules to naturally adsorb onto the TiO_2 particles. All the beakers containing the dyes and the working electrodes were sealed with aluminum foil. The dye-stained TiO_2 film was removed after 24 hours using a thong, and the samples were placed inside different petri dishes with the sensitized surface facing up until the cell assembly [28].

2.7. Preparation of Counter Electrode

The counter electrode was made from another conductive glass. A digital multimeter (DT-830D) was used to check for the conductive face of the glass. A pencil made of lead was used to coat the conductive face of the glass substrate. No masking tape was required for the two parallel edges of this electrode, and thus the whole surface was coated.

2.8. Assembly of Dye-Sensitized Solar Cells (DSSCs)

The liquid electrolyte solution was prepared by dissolving 0.5M potassium iodide salt (KI) and 0.05M iodide (I_2) into acetonitrile [26]. Each dye-sensitized TiO2 electrode sample was placed on a laboratory table so that the deposited film side faced up. The counter electrode was placed on top so that the conductive side of the counter electrode made direct contact with the TiO_2 film. The two opposing glass slides were offset such that all of the TiO_2 was covered by the counter electrode, and about 0.2cm from the two parallel edges of the part of the glass not coated with TiO_2 was exposed. Crocodile clips were used to hold the two parallel edges of the glass slides. The liquid iodide redox electrolyte was injected through the edges of the slides from a complete dye sensitized solar cell [29].

3. Results and Discussion

3.1. Optical Analysis

Figure 1a shows the absorbance result of the roselle (anthocyanin) based cell, bitter leaf (chlorophyll) based cell and a co-sensitized based cell at 0.01 mol nickel doping. The deposited films exhibited a moderate absorbance, with the bitter leaf-based cell and the co-sensitized cell having a pick absorbance value of 0.40 nm in the UV region, which dropped sharply as they moved towards the NIR region of the electromagnetic spectrum, suggesting the dye synergic absorption effect as a result of co-sensitization [28]. It can also be seen that the roselle-based cell exhibited a broad absorption pick at 557 nm, while the bitter leaf and the co-sensitized-based cells exhibited a sharp pick at 665 nm and 676 nm, respectively. This agrees with the results, which show that chlorophyll's pick absorbance is 400-450 nm and 650-700nm, while anthocyanin has a typical absorption band at 400-500 nm. The chlorophyll-based dye, the anthocyanin-based cell and the co-sensitized based cell displayed a high transmittance value of 100%. However, this was followed by a sharp decline to 60% and 50% for the chlorophyll and co-sensitized cells. The anthocyanin(roselle) based cell also observed a decline in transmittance to 78%, all in the visible region of the

electromagnetic spectrum, as shown in figure 1b. Also, it can equally be observed from figure 1c that all the samples revealed a very low reflectance in the visible region of the electromagnetic spectrum. This feature makes the chlorophyll and co-sensitized based cells a more suitable material to be explored as window layers in solar cell fabrication. The observed decrease in transmittance for the chlorophyll and the co-sensitized based dyes, which occurred within the visible region from 600-780 nm, may be attributed to the increased scattering of photons by structural or phase defects in the crystal structure of the films created by doping. [30].

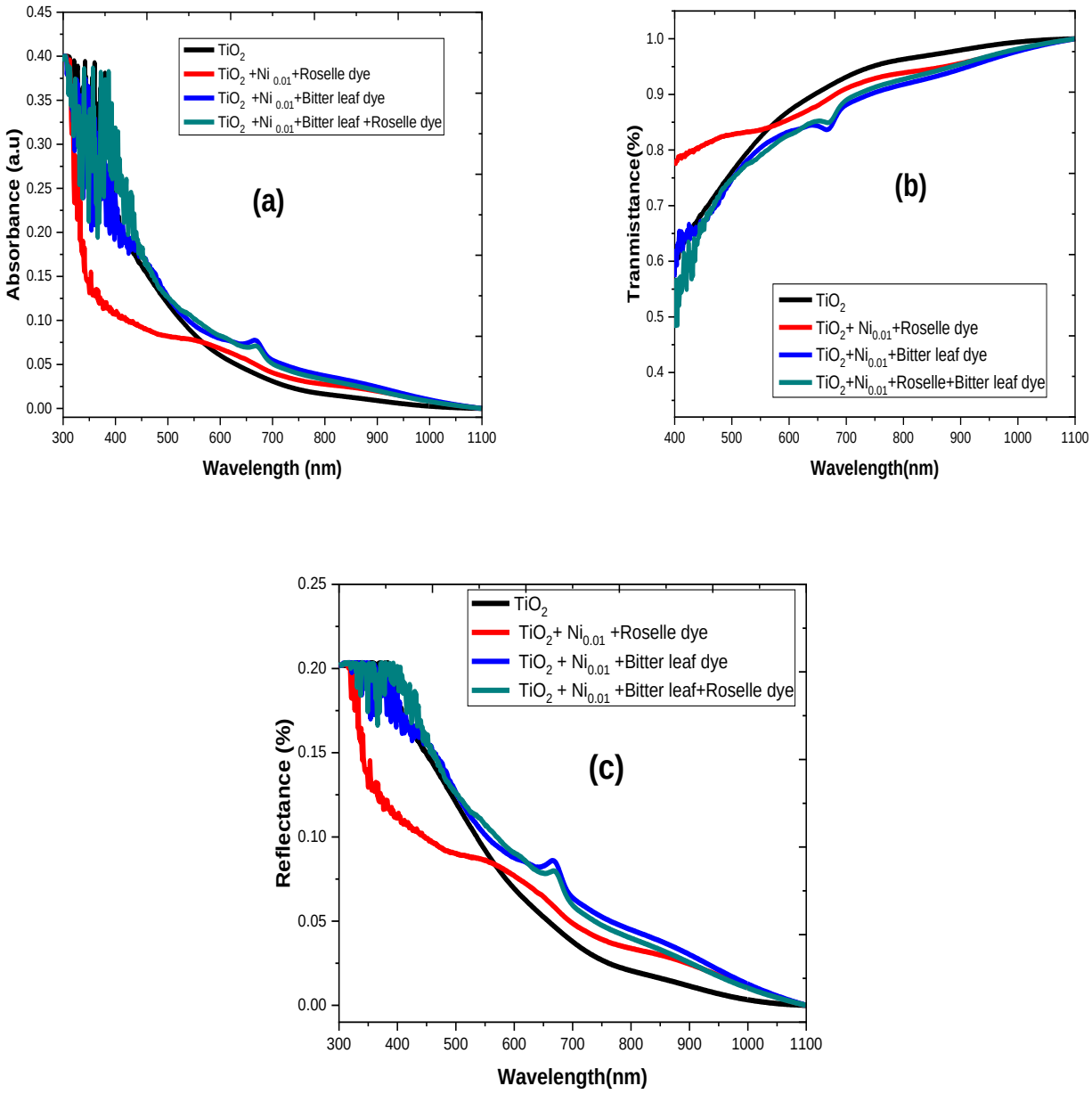

Fig. 1 (a) absorbance, (b) transmittance, and (c) reflectance

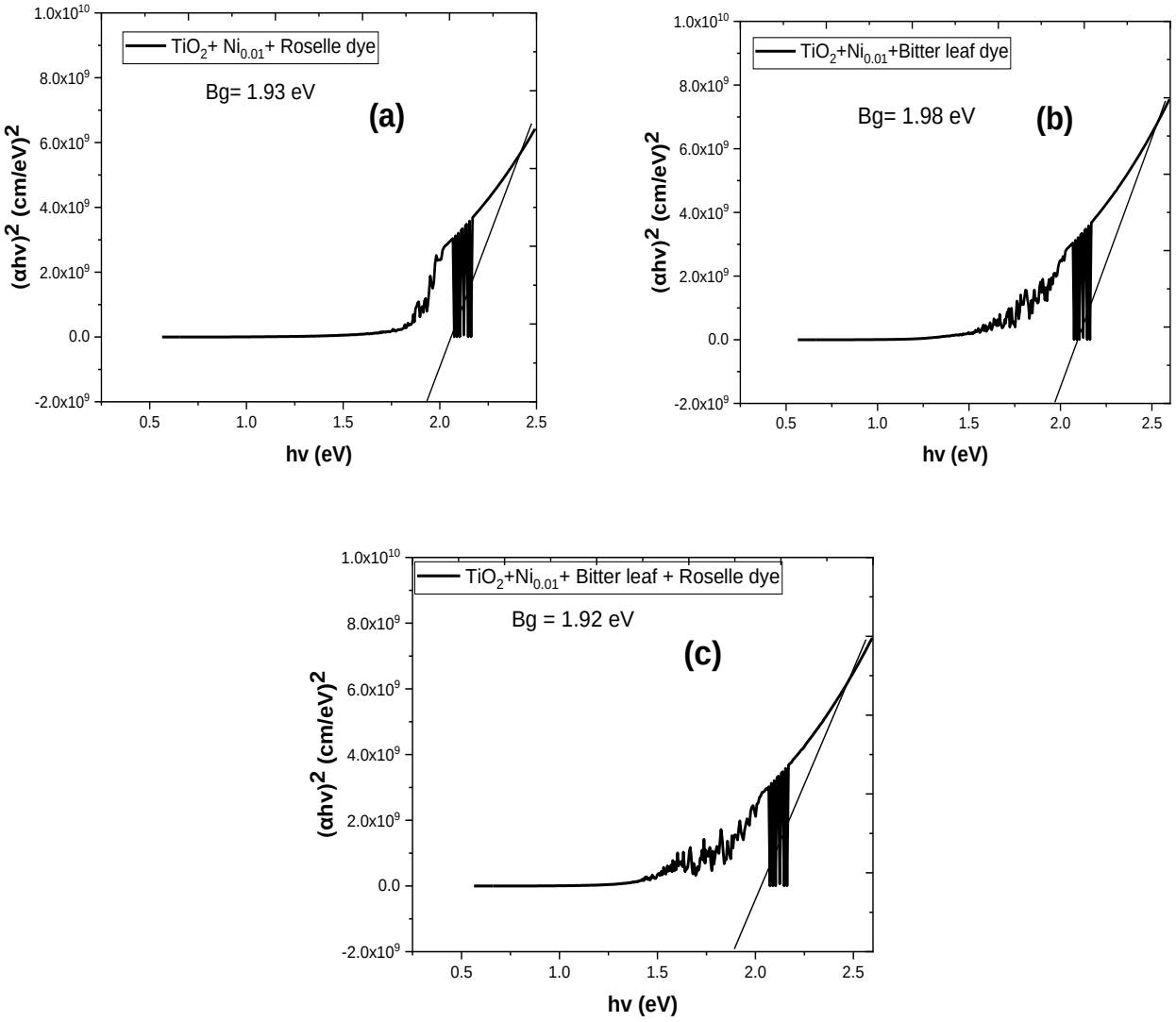

Fig. 2 Optical energy bandgap plots of (a) bitter leaf, (b) roselle, and (c) co-sensitized cells at 0.01mol nickel doping.

3.2. Bandgap Energy

The optical energy bandgap of the bitter leaf (chlorophyll) based cell, roselle (anthocyanin) based cell and the co-sensitized cell were all estimated by extrapolation of the linear portion of the Tauc plots as seen in figure 2 (a, b and c) and summarized in (Table 3). The Tauc plot is one method of determining the optical band gap in semiconductors [31], and this is achieved by plotting the square of the product of the absorption coefficient and photon energy against photon energy. From the result, the optical band gap energy was observed to decrease from 1.98 eV for the chlorophyll-based dye to 1.93 eV for the anthocyanin and 1.92 eV for the co-sensitized dye.

3.3. Surface morphology of the chlorophyll-based dyes and the co-sensitized cells:

Figure 3 shows the Scanning Electron SEM results of the chlorophyll-based cell and the co-sensitized cell at 1μm magnification. For the chlorophyll-based cell (TiO_2, TiO_2+$Ni_{0.01}$+roselle, and TiO_2+$Ni_{0.01}$+roselle+bitter leaf dye), it can be seen that the surface appears smooth, homogenous and has a firmly packed grain-like particle. However, for the co-sensitized dye (TiO_2+$Ni_{0.01}$+bitter leaf dye), the surface appears like that of a nanotube. It could be due to the synergic absorption effect of both dyes. Figure 5 is the EDX spectrum of the synthesized cell; the peaks show that titanium, nickel, oxygen and other element an evident in the synthesized cell.

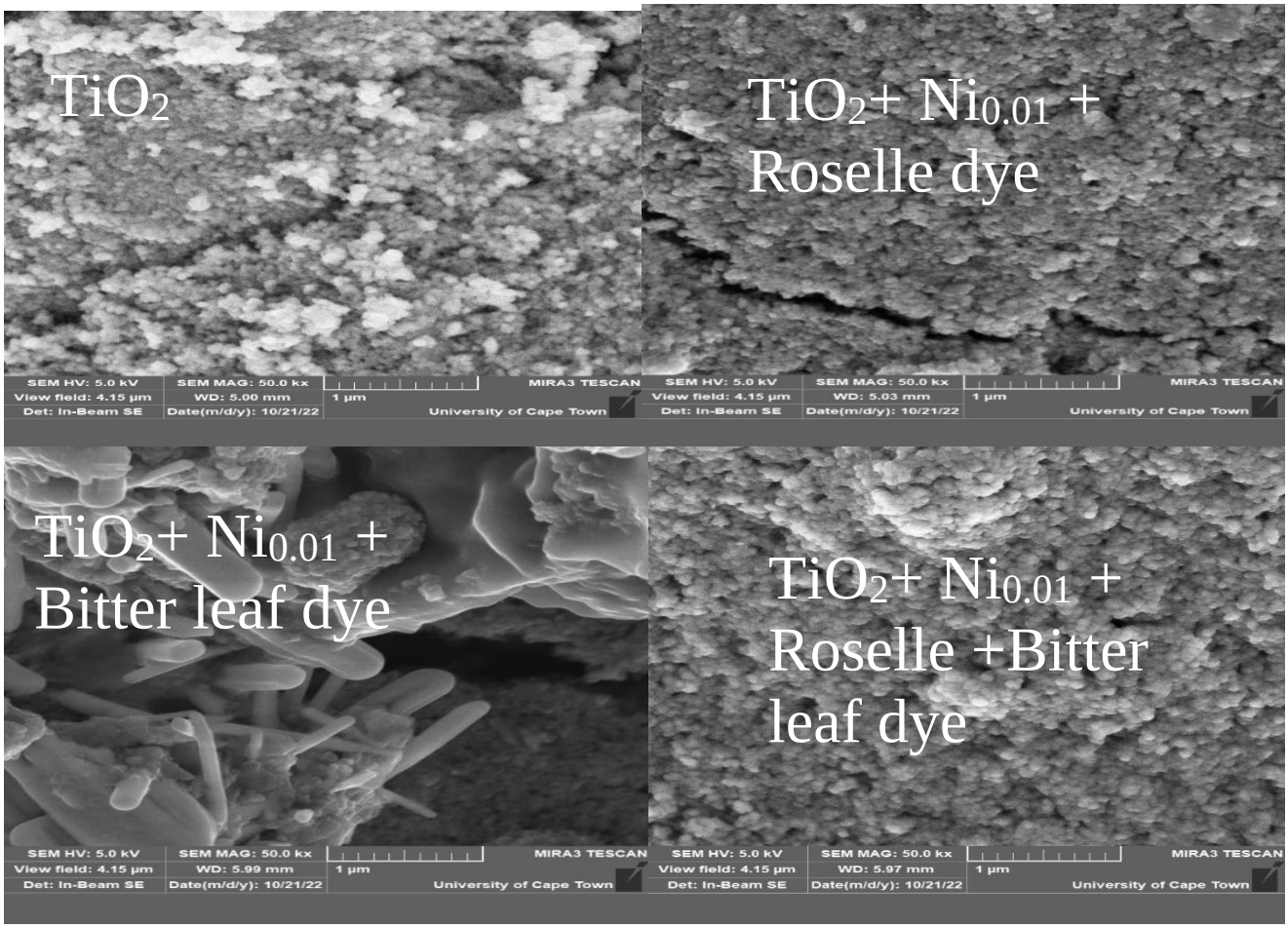

Fig. 3 SEM micrographs of bitter leaf and co-sensitized cells at 0.01 mol nickel doping

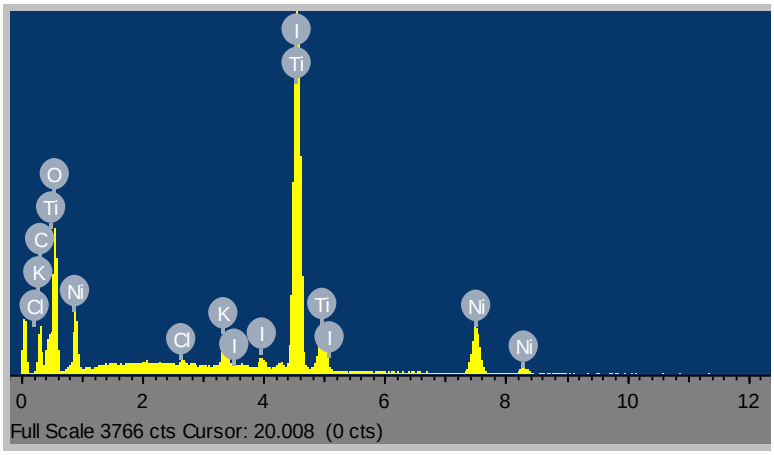

Fig. 4 EDX spectrum of co-sensitized cells at 0.01mol nickel doping.

3.4. Structural analysis of the chlorophyll-based dyes and the co-sensitized dyes

Figure 5 shows the XRD pattern of Titanium dioxide (TiO_2). The XRD pattern showed irregular polycrystalline thin films with fairly randomly oriented peaks. Intense and narrow peaks were seen at (110) and (311) orientation for the film corresponding to 2θ values of 25.34º and 68.77º, respectively. These diffraction angles confirm that a film is an anatase form of TiO_2. Other prominent peaks were also observed to be present in all the spectrums. The peak corresponding to 2θ value of 27.51°, 31.34°, 37.92°, 48.13°, and 54.15° was observed. The lattice parameters obtained from the XRD

pattern are summarized in (Table 1). XRD spectra revealing the structural behavior of the chlorophyll and the co-sensitized cells at the diffraction planes (101), (110), (111), (112), (200), (201), (300), and (311) are as shown in figure 5. The result confirms that all the dye samples have a polycrystalline structure, and their corresponding peaks align with the hexagonal structure [30].

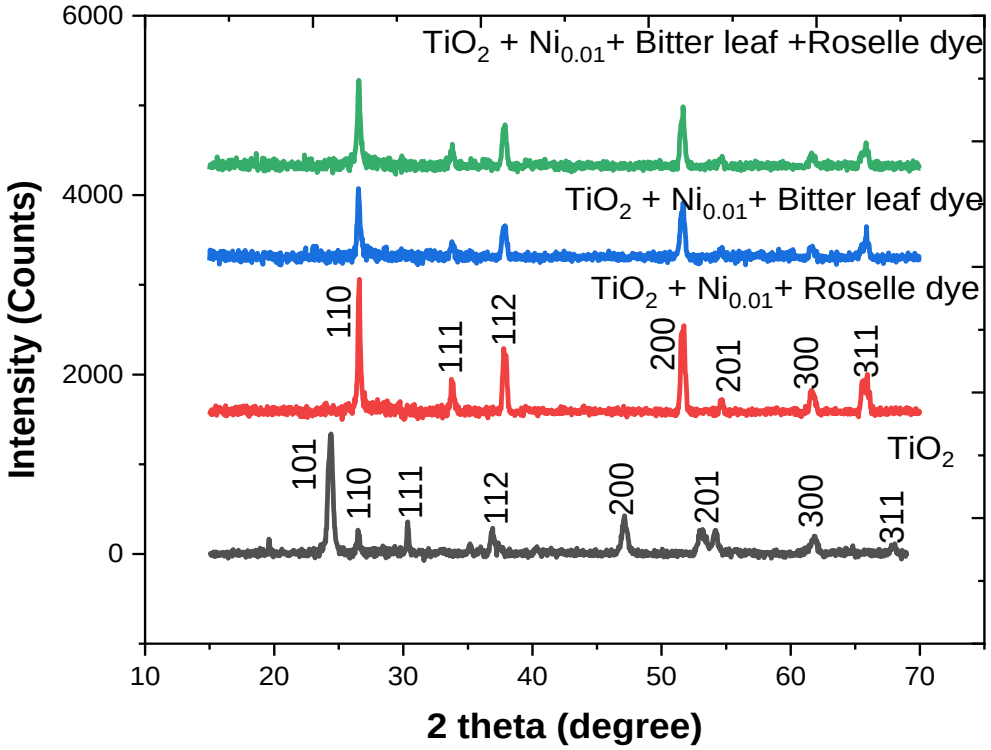

Fig. 5 XRD spectra of bitter leaf and co-sensitized dyes at 0.01mol nickel doping.

Table 1. Structural parameter for TiO_2

Angle (2θ)	FWHM (β)	Crystalline Size, D (nm)	Latice spacing, d (nm)	Dislocation density, δ
25.37	0.2344	2.1565	3.5078	2.15026
27.51	0.2452	3.3993	3.2392	8.6536
31.34	0.2342	5.5338	2.8515	3.2654
37.92	0.2765	2.3172	2.3707	1.8623
48.13	0.2986	2.1174	1.8889	2.2303
54.15	0.2873	1.5161	1.6922	4.3505
62.25	0.2432	2.3413	1.6637	1.8241
68.77	0.2134	1.8690	1.4790	2.8625

Table 2. Structural parameter for bitter leaf and co-sensitized dyes at 0.01mol nickel doping

Angle (2θ)	FWHM (β)	Crystalline Size, D (nm)	Latice spacing, d (nm)	Dislocation density, δ
26.79	0.20452	5.7584	3.3246	1.2889
33.93	0.28618	5.2792	2.6396	1.2460
38.08	0.17913	4.7218	2.3609	1.2170
51.94	0.23884	3.9329	1.7588	1.1008
54.75	0.38006	4.1030	1.6750	7.5299
61.85	0.33022	4.2389	1.4987	7.0268
65.76	0.2254	4.0128	1.4187	4.6456

3.5. Photoelectric Conversion Efficiency of the Chlorophyll, Anthocyanin and Co-sensitized cells

Figure 6 shows the J-V plots for the chlorophyll, anthocyanin and co-sensitized cells, respectively. The I-V characterizations of the cells were measured under illumination intensity using a solar simulator. The illumination intensity used was 881mW/cm^2. The values for the maximum current, Jmp and maximum voltage, Vmp, were obtained from the current density plots and power as a function voltage. The fill factor, FF, a figure of merit for the solar cell, and the solar cell photoelectric conversion efficiency were measured using the following equations according to [26].

$$FF = \frac{V_{mp}\, J_{mp}}{V_{oc} I_{sc}} = \frac{P_m}{V_{oc} I_{sc}} \quad (1)$$

The solar cell photoconversion efficiency is given by

$$\eta = \frac{V_{oc} I_{sc} FF}{p_{in}} \quad (2)$$

The cell parameters and efficiencies of the chlorophyll, anthocyanin and co-sensitized dyes were summarized in table 4. It is observed that for the two lone sensitizers, the chlorophyll (bitter leaf) based cell gave a better efficiency of 0.40%, while the anthocyanin-based cell achieved 0.31% efficiency. The lower efficiency for the anthocyanin-based cell agrees with the result of [28]. The observed differences in efficiency for the two lone dyes could be attributed to their different anchoring functional groups. However, the co-sensitized based cell achieved the highest conversion efficiency of 1.63%, suggesting a dye synergic absorption effect as a result of co-sensitization. It also indicates that 0.01mol of the nickel dopant increases the electrical characteristics of the combined dyes [32]

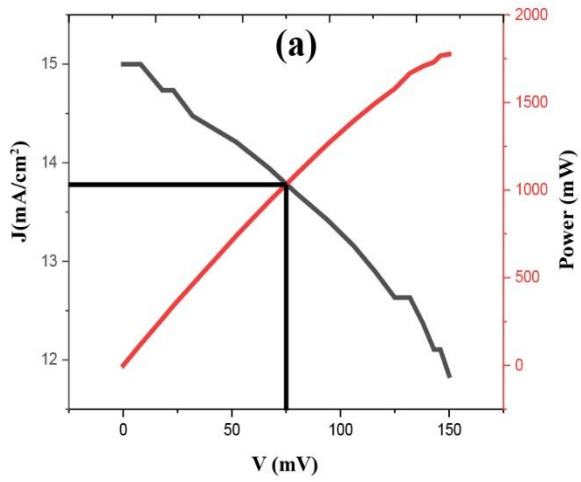

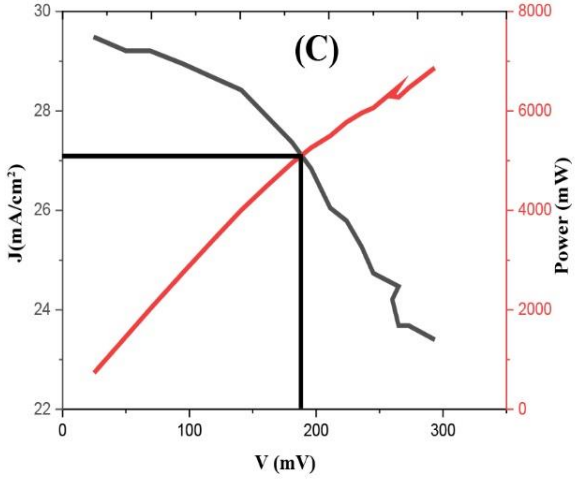

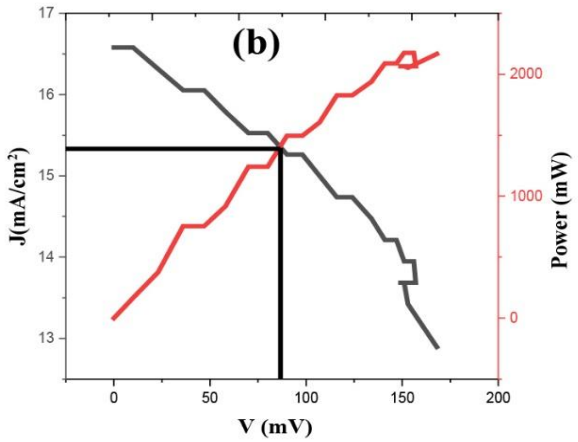

Fig. 6 The J-V curve for cells sensitized with (a) roselle, (b) bitter leaf, (c) roselle and bitter leaf (chlorophyll) dye (co-sensitization) dye under light at 881mW/cm^2

Table 3. Bandgap energy and thickness of roselle, bitter leaf and co-sensitized based dyes.

Sample	Thickness (nm)	Eg(eV)
Roselle based dye	108.01	1.93
Bitter leaf-based dye	110.00	1.98
Co-sensitized dye	107.05	1.92

Table 4. Short circuit current density (J_{sc}), Open circuit voltage (V_{oc}), Maximum voltage (V_{mp}), Maximum current density (J_{mp}), Fill factor (FF), and efficiency (η) of roselle, bitter leaf and co-sensitized dyes.

Sample	J_{sc}(mA/cm^2)	V_{oc} (v)	V_{mp}(v)	J_{mp}(mA/cm^2)	FF (%)	η
Roselle based dye	15.00	155.00	75.00	13.778	0.44	0.31
Bitter leaf-based dye	16.58	170.00	86.166	15.334	0.45	0.40
Co-sensitized dye	29.47	295.00	187.85	27.09	0.58	1.63

4. Conclusion

The fabrication of natural dye sensitized solar cells have been successfully completed using Dr. Blade's deposition method. Natural dyes based on chlorophyll and anthocyanin pigments extracted from bitter leaf and roselle leaf using ethanol as the extraction solvent was used as the photosensitizer for dye sensitized solar cells application. The dyes were used individually as lone sensitizers harnessing the chlorophyll and anthocyanin and co-sensitizers harnessing the combined dyes. 0.01mol nickel was used as the dopant for both the lone dyes and the co-sensitized dye. A comparative study was done for the DSSCs, and their optical behavior was investigated using UV-Vis (UV-1800) spectrophotometer. It was seen that all the nickel-doped dyes showed a moderate absorption peak of 40% in the UV-Vis region of the electromagnetic spectrum. We can now conclude that combined chlorophyll and anthocyanin-based dyes with the highest conversion efficiency of 1.63% and the least energy band gap of 1.92 eV are more efficient than the two lone dyes with efficiencies of 0.31% and 0.40% for the anthocyanin and chlorophyll-based dyes respectively. The observed high efficiency of the co-sensitized dyes implies the dye synergic absorption effect due to co-sensitization. It also suggests that 0.01mol of the nickel dopant increases the electrical characteristics of the combined dyes.

References

[1] Martin A. Green et al., "Solar Cell Efficiency Tables (version 51)," *Progress in Photovoltaics Research and Applications*, vol. 26, no. 1, pp. 3–12, 2018. *Crossref*, https://doi.org/10.1002/pip.2978

[2] Muhammad Shakeel ahmad, A.K. Pandey, and Nasrudin Abd Rahim, "Advancements in the Development of TiO2 Photoanodes and its Fabrication Methods for Dye Sensitized Solar Cell (DSSC) Applications. A Review," *Renewable and Sustainable Energy Reviews*, vol. 77, pp. 89–108, 2017. *Crossref*, https://doi.org/10.1016/j.rser.2017.03.129

[3] Siti nur Fadhilah Zainudin, Huda Abdullah, and Masturah Markom, "Electrochemical Studies of Tin Oxide Based-Dye-Sensitized Solar Cells (DSSC): A Review," *Journal of Materials Science : Materials in Electronics,* vol. 30, no. 6, pp. 5342–5356, 2019. *Crossref,* https://link.springer.com/article/10.1007/s10854-019-00929-6

[4] Yameng Ren et al., "Stable Blue Photosensitizer for Color Palette of Dye-Sensitized Solar Cells Reaching 12.6% Efficiency," *Journal of the American Chemicall Society,* vol. 140, no. 7, pp. 2405–2408, 2018. *Crossref,* https://doi.org/10.1021/jacs.7b12348

[5] Feiyue Huang et al., "Fast Fabricated High Performance Antisolvent-free Perovskite Solar Cells Via Dual-Flash Process," *Electrochimica Acta,* vol. 259, pp. 402–409, 2018. *Crossref,* https://doi.org/10.1016/j.electacta.2017.10.143

[6] N. Prabavathy et al., "Enhancement in the Photostability of Natural Dyes for Dye-Sensitized Solar Cell (DSSC) Applications: A Review," *International Journal of Energy Research,* vol. 41, p. 1372–1396, 2017. *Crossref,* https://doi.org/10.1002/er.3703

[7] P.N. Anggraini, L. Retnaningsih, and J. Hidayat, "Reliability Performance of Up-Scaling DSSC into Sub-Module in Series Design Using Hermetic Sealing," *Journal of Physics:Conference Series, IOP Publishing,* vol. 985, p. 012052, 2018. *Crossref,* https://doi.org/10.1088/1742-6596/985/1/012052

[8] Brain O'Regan, and Michael Grätzel, "A Low-Cost, High-Efficiency Solar Cell Based on Dye-Sensitized Colloidal TiO2 Films," *Nature,* vol. 353, pp. 737–740, 1991. *Crossref,* https://doi.org/10.1038/353737a0

[9] Syed Ghufran Hashmi et al., "High Performance Dye-Sensitized Solar Cells With Inkjet Printed Ionic Liquid Electrolyte," *Nano Energy,* vol. 17, pp. 206–215, 2015. *Crossref,* https://doi.org/10.1016/j.nanoen.2015.08.019

[10] Paolo Mariani, Luigi Vesce, and Aldo Di Carlo, "The Role of Printing Techniques for Large-Area Dye Sensitized Solar Cells," *Semiconductor Science and Technology,* vol. 30, no. 10, p. 104003, 2015. *Crossref,* https://doi.org/10.1088/0268-1242/30/10/104003

[11] E. Kouhestanian et al., "Electrodeposited ZnO Thin Film as an Efficient Alternative Blocking Layer for TiCl4 Pretreatment in TiO2-Based Dye Sensitized Solar Cells," *Superlattices and Microstructures,* vol. 96, pp. 82–94, 2016. *Crossref,* https://doi.org/10.1016/j.spmi.2016.05.012

[12] Ladislav Kavan, Ludmilla Steier, and Michael Grätzel, "Ultrathin Buffer Layers of SnO2 by Atomic Layer Deposition: Perfect Blocking Function and Thermal Stability," *Journal of Physical Chemistry,* vol. 121, no. 1, pp. 342–350, 2016. *Crossref,* https://doi.org/10.1021/acs.jpcc.6b09965

[13] T. Marimuthu et al., "Facile Growth of ZnO Nanowire Arrays and Nanoneedle Arrays with Flower Structure on ZnO-TiO2 Seed Layer for DSSC Applications," *Journal of Alloys and Compounds,* vol. 693, p. 1011–1019, 2017. *Crossref,* https://doi.org/10.1016/j.jallcom.2016.09.260

[14] Kailas K. Tehare et al., "Enhanced DSSCs Performance of TiO2 Nanostructure by Surface Passivation Layers," *Materials Research Bulletin,* vol. 99, pp. 491–495, 2018. *Crossref,* https://doi.org/10.1016/j.materresbull.2017.11.046

[15] Solomon Offiah et al., "Study of the Extrinsic Properties of ZnO:Al Grown by SILAR Technique," *Journal of Solid State Electrochemistry,* vol. 21, no. 9, pp. 2621-2628, 2017. *Crossref,* https://link.springer.com/article/10.1007/s10008-017-3514-6

[16] Qamar Wali et al., "SnO2–TiO2 Hybrid Nanofibers for Efficient Dye-Sensitized Solar Cells," *Solar Energy,* vol. 132, p. 395–404, 2016. *Crossref,* https://doi.org/10.1016/j.solener.2016.03.037

[17] Masoud Abrari et al., "Fabrication of Dye-Sensitized Solar Cells Based on SnO2/ZnO Composite Nanostructures: A new Facile Method Using Dual Anodic Dissolution," *Journal of Alloys Compounds,* vol. 784, pp. 1036–1046, 2019. *Crossref,* https://doi.org/10.1016/j.jallcom.2018.12.299

[18] E. N. Nunes et al., "Nb2O5 dye-sensitized solar cells," *Nanomaterials for Solar Cell Applications,* pp. 287–322, 2019.

[19] Xiaomin Yang et al., "Mixed-steam Annealing Treatment for Perovskitefilms to Improve Solar Cells Performance," *Solar Energy,* vol. 177, p. 299–305, 2019. *Crossref,* https://doi.org/10.1016/j.solener.2018.11.005

[20] Niyamat I. Beedri et al., "Bilayered ZnO/Nb2O5 Photoanode for Dye Sensitized Solar Cell," *International Journal of Modern Physics,* vol. 32, no. 19, p. 1840046, 2018. *Crossref,* https://doi.org/10.1142/S0217979218400465

[21] Abdelhafed Taleb et al., "Optimized TiO2 Nanoparticle Packing for DSSC Photovoltaic Applications," *Solar Energy Material and Solar Cells,* vol. 148, pp. 52–59, 2016. *Crossref,* https://doi.org/10.1016/j.solmat.2015.09.010

[22] Brian O'regan, and Michael Grätzel, "A Low-Cost, High-Efficiency Solar Cell Based on Dye-Sensitized Colloidal TiO2 Films," *Nature,* vol. 353, pp. 737-740, 1991. *Crossref,* https://doi.org/10.1038/353737a0

[23] Mark Z. Jacobson, "Review of Solutions to Global Warming, Air Pollution, and Energy Security," *Energy & Environmental Science*, vol. 2, no. 2, pp. 148-173, 2008. *Crossref,* https://doi.org/10.1039/B809990C

[24] Georges Makhoul, Hafez Mahfoud, and Hussam Baroudi, "Some Chemical Characteristics of White (Morus Alba L) and Black (Morus Nigra L) Mulberry Phenotypes in Tartus Syria," *SSRG International Journal of Agriculture & Environmental Science*, vol. 4, no. 2, pp. 53-62, 2017. *Crossref,* https://doi.org/10.14445/23942568/IJAES-V4I2P110

[25] Philip Jackson et al., "Effects of Heavy Alkali Elements in Cu (In, Ga) Se2 Solar Cells with Efficiencies up to 22.6%," *Physica Status Solidi –Rapid Research Letters,* vol. 10, no. 8, pp. 583-586, 2016. *Crossref,* https://doi.org/10.1002/pssr.201600199

[26] P.O Isi, A.J. Ekpunobi, and D.N. Okoli, "Optical and Electrical Properties of Fabricated Solar Cells Based on Extract from Bush Tea (hyptis suaveolens)," *International Organization of Scienctific Research Journal of applied physics (IOSR-JAP)*, vol. 13, no. 4, pp. 01-07, 2021. *Crossref*, https://doi.org/10.9790/4861-1304010107

[27] Jude O. Ozuomba, Laetivis U. Okoli, and Azybuike J. Ekpunobi, "The performance and stability of Anthocyanin Local Dye as a Photosensitizer for DSSCs," *Advances in Applied Science Research*, vol. 4, no. 2, pp. 60-69, 2013.

[28] K. U. Isah, A.Y. Sadik, and B.J. Jolayemi, "Effect of Natural Dye Co-Sensitization on the Performance of Dye-Sensitized Solar Cells (DSSCs) Based on Anthocyanin and Betalain Pigments Sensitization," *European Journal of Applied Science*, vol. 9, no, 3, pp. 140-146, 2017. *Crossref*, https://doi.org/10.5829/idosi.ejas.2017.140.146

[29] Harasai Setyawati et al., "Effect of Metal ion Fe (III) on the Performance of Chlorophyll as Photosensitizers on Dye Sensitized Solar Cell," *Results in Physics*, vol. 7, pp. 2907-2918, 2017. *Crossref*, https://doi.org/10.1016/j.rinp.2017.08.009

[30] Imosobomeh L. Ikhioya, Nwamaka I. Akpu, and Faith U. Ochai-Ejeh, "Influence of Erbium (Er) Dopant on the Enhanced Optical Properties of Electrochemically Deposited Zinc Oxide (ZnO) Films for High-Performance Photovoltaic Systems," *Optik*, vol. 252, p. 168486, 2022. *Crossref*, https://doi.org/10.1016/j.ijleo.2021.168486

[31] P. R Jubu et al., "Tauc-Plot Scale and Extrapolation Effect on Bandgap Estimation from UV–Vis–NIR Data–a Case Study of B-Ga2O3," *Journal of Solid State Chemistry*, vol. 290, p. 121576, 2020. *Crossref*, https://doi.org/10.1016/j.jssc.2020.121576

[32] Handoko Darmokoesoemo et al., "Synthesis of Complex Compounds Ni (II)-Chlorophyll as Dye Sensitizer in Dye Sensitizer Solar Cell (DSSC)," *Korean Chemical Engineering Research*, vol. 55, no. 1, pp. 19-26, 2017. *Crossref*, http://dx.doi.org/10.9713/kcer.2017.55.1.19

[33] Nwamaka I. Akpu et al., "Investigation on the Influence of Varying Substrate Temperature on the Physical Features of Yttrium Doped Cadmium Selenide Thin Films Materials," *SSRG International Journal of Applied Physics*, vol. 8, no. 2, pp. 37-46, 2021. *Crossref*, https://doi.org/10.14445/23500301/IJAP-V8I2P106

[34] Imosobomeh L. Ikhioyaa et al., "Effect of Precursor pHon Cadmium Doped Manganese Sulphide (CdMnS) Thin Films for Photovoltaic Application," *SSRG International Journal of Applied Physics*, vol. 6, no. 2, pp. 1-8, 2020. *Crossref*, https://doi.org/10.14445/23948884/IJMSE-V6I2P101

[35] Imosobomeh Lucky Ikhioya, Okoli D. N, and Ekpunobi A. J, "Effect of Temperature on SnZnSe Semiconductor Thin Films for Photovoltaic Application," *SSRG International Journal of Applied Physics*, vol. 6, no. 2, pp. 55-67, 2019. *Crossref*, https://doi.org/10.14445/23500301/IJAP-V6I2P109

[36] Imosobomeh Lucky Ikhioya et al., "The Influence of Precursor Temperature on the Properties of Erbium-Doped Zirconium Telluride Thin Film Material via Electrochemical Deposition," *SSRG International Journal of Applied Physics*, vol. 7, no. 1, pp. 102-109, 2020. *Crossref*, http://dx.doi.org/10.14445/23500301/IJAP-V7I1P115

[37] Imosobomeh Lucky Ikhioya, and Azubike Josiah Ekpunobi, "Effect of Deposition Period and pH on Electrodeposition Technique of Zinc Selenide Thin Films," *Journal of Nigeria Association of Mathematical Physics*, vol. 28, no. 2, pp. 281-288, 2014.

[38] Imosobomeh Lucky Ikhioya, and Azubike Josiah Ekpunobi, "Electrical and Structural properties of ZnSe Thin Films by Electrodeposition Technique," *Journal of Nigeria Association of Mathematical Physics*, vol. 29, pp. 325-330, 2015.

[39] Imosobomeh Lucky Ikhioya, Ugbo F. C, and Ijabor B. Okeghene, "Growth and Characterization of Manganese Sulphide (MnS) Thin Films," *International Journal for Research in Applied and Natural Science*, vol. 4, no. 1, pp. 1-9, 2018. *Crossref*, https://doi.org/10.53555/ans.v4i1.77

[40] Imosobomeh Lucky Ikhioya, Goodfriend M. Whyte, and Agnes C.Nkele, "Temperature-Modulated Nanostructures of Ytterbium-Doped Cobalt Selenide (Yb-CoSe) for Photovoltaic Applications," *Journal of the Indian Chemical Society*, vol. 100, no. 1, p. 100848, 2023. *Crossref*, https://doi.org/10.1016/j.jics.2022.100848

[41] Kufre I. Udofia et al., "Effects of Zirconium on Electrochemically Synthesized Tin Selenide Materials on Fluorine Doped Tin Oxide Substrate for Photovoltaic Application," *Journal of the Indian Chemical Society*, vol. 99, no. 10, p. 10077, 2022. *Crossref*, https://doi.org/10.1016/j.jics.2022.100737

[42] Omar Ellabban, Haitham Abu-Rub, and Frede Blaabjerg, "Renewable Energy Resources: Current Status, Future Prospects and Their Enabling Technology," *Renewable and Sustainable Energy Reviews*, vol. 39, pp. 748-764, 2014. *Crossref*, https://doi.org/10.1016/j.rser.2014.07.113